IJE TRANSACTIONS B: Applications Vol. 34, No. 05, (May 2021) 1195-1212

International Journal of Engineering

Journal Homepage: www.ije.ir

Retrofitting of RC Beams using Reinforced Self-compacting Concrete Jackets Containing Aluminum Oxide Nanoparticles

A. Faez, A. Sayari*, S. Manie

Civil Engineering Department, Sanandaj Branch, Islamic Azad University, Sanandaj, Iran

PAPER INFO

Paper history:
Received 27 December 2020
Received in revised form 14 March 2021
Accepted 15 March 2021

Keywords:
Aluminum Oxide Nanoparticles
Finite Element Method
Reinforced Concrete Jacket
Retrofitting

ABSTRACT

The purpose of this study was to introduce a proposed method to retrofit RC beams. For this purpose self-compacting concrete containing aluminium oxide nanoparticles (ANPs) and silica fume (SF) was used in RC jackets. The laboratory experiment and numerical simulation were used to investigate the behavior of the beams. The experimental variables were included the amount of ANPs used in the jackets (0 and 2.5% by weight of cement) and the surface interaction between beam and jacket (75% and 100% of the side and bottom surfaces of the beam). Five RC beams with a length of 1.4 m and the same dimensions were made and subjected to four-point loading. After completing the laboratory steps, RC beams were simulated according to laboratory conditions using the finite element method and ABAQUS software. After verifying the used method, parametric analysis was performed and parameters such as beam span length (1.5, 3, 4.5 m), concrete jacket thickness (4, 8, and 12 cm), and the diameter of the bars used in the jacket (8, 10 and 12 mm) were examined. The results showed that the use of RC jackets containing ANPs, depending on the jacket thickness, the diameter of the bars used in the jacket, and the length of the beam span increased the beams flexural strength by 155 to 447%. It was observed that the crushing of concrete without nanoparticles compared to concrete contain nanoparticles is more severe because nanoparticles affected the concrete matrix and reduced its crushing in RC jackets.

***doi**: 10.5829/ije.2021.34.05b.13*

1. INTRODUCTION

In recent years, following the deterioration of building structures and the need for retrofitting structures to satisfy the strict design requirements, much emphasis has been placed on repairing buildings [1–3]. One of the methods that can prevent the loss of materials as much as possible and reduce construction debris is retrofitting of buildings [4–6]. Increasing the strength of the structure is very important during the retrofitting because this will increase the useful life of the structure and residents will feel more secure [7–9]. Various studies have been conducted on retrofitting of RC beams. Sangi et al. [10] made 35 self-compacting concrete beams and retrofitted them with CFRP sheets in the tensile zone (bottom surface of the beam). Also, numerical simulation was used to investigate the fracture mode and cracks distribution in the samples. It was indicated that the retrofitted beam with CFRP angle 0° has more capacity in comparison to other specimens [10]. Shadmand et al. [11] introduced a proposed method for retrofitting RC beams in which steel-concrete composite jackets containing steel fibers were used. For this purpose, 75% of the peripheral surface of RC beams was initially reinforced using steel plates and bolts. Then steel fiber reinforced concrete was used between the steel plates and the perimeter of the beam. The results showed that steel fiber-reinforced composite jackets delay the formation of the first crack in the concrete and the energy absorption capacity of the beams increased by 89 to 129% depending on the amount of steel fiber [11]. Rahmani et al. [12] investigated the response of retrofitted RC beams with RC jackets containing steel fiber. For this purpose, 25 RC beams with different concrete jackets were made and their bearing capacity was evaluated. The result showed that the use of RC jacket containing steel fiber can increase the bearing capacity of the beams by about 7.4 times in compare to the control beam [12].

*Corresponding Author Email: *Sayari_arash@yahoo.com* (A. Sayari)

Please cite this article as: A. Faez, A. Sayari, S. Manie, Retrofitting of RC Beams using Reinforced Self-compacting Concrete Jackets Containing Aluminum Oxide Nanoparticles, International Journal of Engineering, B: Applications Vol. 34, No. 05, (2021) 1195-1212

On the other hand, nanotechnology development in engineering sciences has been studied by other researchers [13, 14]. The disadvantages of increasing cement production have led to use of nanoparticles in concrete. Nanoparticles can improve the concrete properties and reduce cement consumption in different countries [15–17]. The nanoparticles are usually used in concrete in powder form or distributed in solution [18–20]. The most important used nanoparticles are titanium nanoparticles (TiO_2), aluminium nanoparticles (Al_2O_3), silica nanoparticles (SiO_2), iron nanoparticles (Fe_2O_3), and clay nanoparticles (Nano-Clay) [21–23]. Among the mentioned particles, aluminum oxide nanoparticles (ANPs) are one of the important ceramic materials that have various applications in various fields [24–26]. Li et al. [27] investigated the effect of ANPs in cement mortar. The results showed that by adding 5% ANPs, the concrete elasticity modulus increased by 143% [27]. Oltulu and Sahin [28] investigated the effect of Nano silica, ANPs, and iron oxide nanoparticles separately and in combination with fly ash and silica fume. The results showed that the best performance in terms of compressive strength and permeability was obtained in the presence of 1.25% ANPs [10]. Behfarnia and Salemi [29] investigated the effects of nano silica particles and ANPs on the resistance of ordinary concrete to freezing. The results showed that the freezing resistance of concrete containing nanoparticles is significantly improved due to the dense structural creation [29]. Ismael et al. [30] investigated the effect of nano silica and ANPs additives on the adhesion between steel and concrete. The results indicated that nanoparticles increased the adhesion between steel and concrete [30]. Niewiadomski et al. [31] investigated the properties of self-compacted concrete (SCC) modified with nanoparticles. The results showed that the fluidity of concrete decreases with increasing amounts of ANPs and silica nanoparticles. Also, the hardness values and elasticity modulus of the samples containing nanoparticles were higher compared to the samples without nanoparticles [31]. Ghazanlou et al. [32] investigated the mechanical properties of cementations composites containing iron nano oxide. Cement paste samples were tested with 0.2% iron nano oxide. The results indicated that the use of nanoparticles can increase the tensile strength, flexural strength, and compressive strength of specimens by about 15-19%, 17-25%, and 23-32%, respectively [32]. Heidarzad Moghaddam et al. [33] investigated the effects of ANPs on the mechanical and durability properties of fiber SCC. The results showed that the combined use of 2% ANPs and 1% glass fibers increased the compressive and tensile strengths of SCCs by 59 and 119.2%, respectively [33]. Zeinolabedini et al. [34] investigated ultra–high–performance concrete containing polypropylene fibers and aluminum oxide, nano-lime, and nanosilica. The results showed that the effect of increasing the amount of cement on increasing the flexural strength is much less than increasing the amount of nanomaterials [34]. Muzenski et al. [35] investigated the properties of concrete containing fiber and aluminum oxide nanofibers. The results showed that the combined use of aluminum oxide nanoparticles and fibers can be a good option to improve compressive strength [35].

As mentioned, studies about retrofitting of RC structural elements show that concrete jackets and FRP sheets are the common methods that have been used. Although the FRP method can increase the bearing capacity of the beams, the separation of FRP sheets from concrete surfaces, the weakness against fire, and its different properties from concrete are among the disadvantages that can affect its performance. On the other hand, the concrete used in ordinary RC jackets is weak against tensile stresses and the performance role of the jackets can be improved by using various additives. One of these additives is ANPs. The adhesion between the steel rebars and the used binder in the RC jacket can play a very important role. Studies about the use of ANPs in the concrete show that the use of these materials in concrete increase the adhesion between concrete and rebar, so due to the relatively limited space between the formwork and the old concrete, the use of nanoparticles increase the adhesion between the rebars in the jackets and the surrounding concrete compared to ordinary concrete, and thus the bearing capacity of the RC beam will be higher. ANPs can also improve the heat resistance of concrete due to fire. These materials also affect the durability properties of concrete. Considering the advantages of ANPs in concrete, in the present study, ANPs were used in the concrete jacket to retrofit of RC beam. The study was conducted in two parts: laboratory and software simulation. Improving the performance and increasing the bearing capacity of RC beams using reinforced self-compacting concrete jackets containing ANPs are among the objectives of the present study. Thus, according to the characteristics of nanoparticles, in addition to increasing the energy absorption capacity of RC beams, the use of nanoparticles is effective in reducing the consumption of natural resources and raw materials used in cement production. Also, self-compacting of the concrete used in concrete jackets is another case that causes concrete to be poured completely into the space between the rebars.

2. STUDY PROCESS

Studies were performed in two stages: laboratory and software simulation. In the laboratory part, concrete specimens containing ANPs and SF were made for different percentages, and tests such as slump flow, T50, V-funnel, L-box, compressive strength, splitting tensile strength, and water absorption were performed and the

most optimal mixture design selected. Fresh concrete tests were performed to check the self-compaction properties of the concrete specimens. Rheological, durability, and mechanical properties were investigated in a study conducted by the authors [36]. The mixture design and results of the mentioned study are presented in Tables 1 and 2, receptively. Fresh concrete tests were performed according to EFNARC [37] and compressive and splitting tensile strengths, and water absorption tests were performed according to ASTM C39 [38], ASTM C496 [39], and ASTM C642-13 [40], respectively. After reviewing the results related to determining the mechanical and rheological properties of concretes containing ANPs and SF, five RC beams with the same dimensions and specifications steel reinforcement were made and subjected to four-point loading in the center of the span in conditions with and without retrofitting. The bearing capacity, mid-span deflection, and energy absorption capacity were determined. The studied beams had hinged support and in the state without retrofitting and retrofitted with two different arrangements of the concrete jacket after 28 days were subjected to 4-point loading. The concrete used in the jacket was once conventional and once retrofitted with concrete containing ANPs. After completing the laboratory steps, retrofitted concrete beams with a concrete jacket containing ANPs were simulated using the finite element method (FEM) and ABAQUS software [41] and were subjected to loading according to laboratory conditions, and load-deflection curves were determined. After ensuring the accuracy of the simulation method, which was performed using laboratory studies, the behavior of RC beams retrofitted with the proposed jacket was evaluated by numerical simulation and variables such as beam span length, the jacket thickness, and the diameter of the reinforcement bars used in the jacket were examined.

3. LABORATORY PROGRAM

3. 1. Materials Materials include coarse aggregates, fine aggregates, cement, water, ANPs, SF, and superplasticizers. River sand and crushed gravel were

TABLE 1. Mix design (kg/m^3) [36]

Mix	C	W	SF	S	G	NP	SP
NA0	350	168	35	960	920	0	2.76
NA0.25	314.125	168	35	960	920	0.875	2.86
NA0.50	313.25	168	35	960	920	1.75	2.93
NA0.75	312.375	168	35	960	920	2.625	3.03
NA1	311.5	168	35	960	920	3.5	3.35
NA1.25	310.625	168	35	960	920	4.375	3.46
NA1.50	309.75	168	35	960	920	5.25	3.89
NA1.75	308.875	168	35	960	920	6.125	4.03
NA2	308	168	35	960	920	7	4.12
NA2.25	307.125	168	35	960	920	7.875	4.45
NA2.50	306.25	168	35	960	920	8.75	4.89
NA2.75	375.305	168	35	960	920	9.625	4.92
NA3	304.5	168	35	960	920	10.5	4.65

C: Cement W: Water SF: Silica fume S: Sand
G: Gravel NP: Nanoparticles SP: Superplasticizer

TABLE 2. Results of slump flow, T50, V-funnel, L-box, compressive strength, splitting tensile strength, and water absorption [36]

Mix	Slump flow (mm)	T50 (s)	V-funnel (s)	L-Box (H_2/H_1)	Compressive strength (MPa)			Splitting tensile strength (MPa)			Water absorption (%)
					Days			Days			Days
					7	28	90	7	28	90	28
NA0	749	2.41	6.3	0.97	21.12	26.1	29.31	2.78	2.9	3.6	5.73
NA0.25	746	2.67	6.4	0.94	22.33	28.12	30.92	2.86	2.95	3.79	5.61
NA0.50	737	2.77	6.9	0.91	24.24	33.22	34.11	2.89	3.31	3.85	5.41
NA0.75	733	2.89	7.4	0.88	25.11	35.11	37.11	2.9	3.34	3.92	5.35
NA1	721	3.53	7.7	0.86	26.14	36.21	39.22	2.91	3.41	3.95	5.15
NA1.25	701	3.57	8.3	0.86	26.32	40.12	43.13	2.92	3.41	3.98	4.81
NA1.50	691	3.78	9.19	0.85	27.22	45.11	46.21	2.98	3.43	4.11	4.41
NA1.75	687	4.41	7.971	0.85	28.13	46.21	48.12	3.19	3.86	4.33	3.76
NA2	684	4.51	10.41	0.84	29.22	47.12	50.12	3.39	4.29	5.04	3.12
NA2.25	671	4.57	10.49	0.83	29.91	48.13	51.23	3.41	4.3	5.05	2.85
NA2.50	665	4.59	11.12	0.83	30.91	49.14	54.34	3.6	4.5	5.31	2.83
NA2.75	665	4.68	11.37	0.82	30.12	48.22	53.11	3.5	4.41	5.27	2.79
NA3	663	4.91	11.82	0.82	30.01	47.34	52.12	3.4	4.4	5.21	2.77

used. The density of sand and gravel were 2600 and 2650 kg/m^3, respectively. Sand and gravel grading were conducted according to ASTM C33/C33M-18 [42]. Cement type II was used. The water used in this study is drinking water. ANPs is one of the chemical compounds with the chemical formula Al_2O_3, which has various brands such as alumina, corundum, etc. This material has a very high melting temperature about 2054 degrees Celsius and is very stable chemically. This property allows this material to be used in applications that need high temperatures. Hardness, strength, and abrasion resistance of ANPs are the highest among oxides. The ANPs used in this research have a small size and high activity, in powder form and almost spherical. These nanoparticles have a specific surface area of 138 m^2/g and a density of 3890 kg/m^3 and an average particle size of 20 nm. Also. they are white. The compounds of the used ANPs are presented in literature [36]. The SF is produced by Iran Ferrosilicon factory with a specific weight of 2200 kg/m^3 and a blaine of 20.2 g/m^2, which is added with a dry form to the concrete mix in the amount of 10% by weight of cement. The SF and cement chemical properties are presented in literature [36]. The brand of superplasticizer used is "Zhikaplast" and its specific gravity is 1.10 g/cm^3. Concrete was made using a concrete mixer. First, the coarse aggregates and fine aggregates were mixed in a concrete mixer, half of the mixing water was added and the mixing was continued. At this stage, cement, SF, and 10% water were added to the mixture, and mixing was continued in a concrete mixer. Finally, ANPs and then residual water were added. After mixing, the superplasticizer was gradually to visually feel the fresh self-compacting concrete has achieved the necessary efficiency and homogeneity.

3. 2. Retrofitting of RC Beams using SCC Jacket Containing ANPs and SF After examining the rheological and mechanical properties of concretes containing ANPs and SF, it was concluded that the concrete specimen containing 2.5% ANPs and 10% SF has a better performance compared to other specimens according to tensile and compressive strengths.

The increase in compressive and tensile strengths of NA2.5 compared to the control sample was 88% and 55%, respectively. Also, in terms of workability, the mentioned sample has met all the criteria related to SCCs. Therefore, it was selected as the most optimal mixture design and used in the concrete jackets. The beams had hinged support. Two different arrangements were considered for the proposed jacket. A four-point bending test was used for beam specimens. Mid-span deflection and the corresponding load were recorded. Concretes containing ANPs and without ANPs were used in the jackets in different cases. The geometric characteristics and reinforcement bars details of the beams are present in Figure 1.

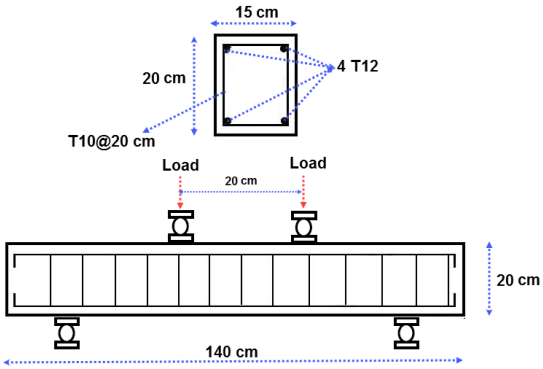

Figure 1. Geometric specifications and steel reinforcement details of the investigated beams

The beam's span length is 120 cm. The schematic arrangement of the investigated jackets is shown in Figure 2. Three sides of the beam were retrofitted due to the typical floor-to-beam connection. The proposed jacket was once placed on 75% of the perimeter and bottom of the beams and once again on 100% perimeter and bottom of beams. A beam was also constructed as a control beam to evaluate the effectiveness of the proposed method. The tested beams are presented in Table 3. According to Figure 2, the thickness of the concrete jacket (t_j) at the sides and bottom of the beam was considered 4 cm. The diameter of the reinforcement bars and the distances between them were considered 10 mm and 50 mm, receptively. The selection of studied beams dimensions and geometric characteristics has been done according to similar studies in which the beams retrofitting have been evaluated. Beam stirrups were made with a stirrup machine. To make and install concrete jacket, voids were made on the beams at intervals of about 20 cm from each other. After removing the dust inside the voids, L-shaped reinforcement bars were placed inside the voids and attached to the beam surfaces using epoxy glue. After that, the reinforcement bar mesh of the jacket was connected to L-shaped reinforcement bar using wire. The jacket reinforcement bar mesh consisted of 10 mm diameter reinforcement bar spaced approximately 5 cm apart. The construction stages of retrofitted beams are shown in Figure 3.

A fully automatic flexural jack with a load capacity of 2000 kN was used to apply loads to the beams. This

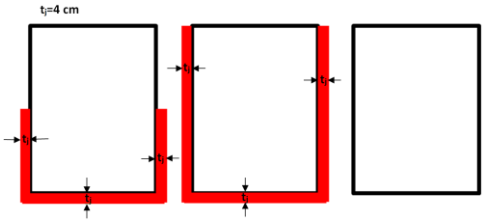

Figure 2. The arrangement of the investigated jackets

TABLE 3. Introducing the tested beams

No.	Name	Additives used in jacket	Description
1	CB	-	Control beam
2	R75	SF	75% of the perimeter surface and the lower part of the beam
3	R100	SF	100 % of the perimeter surface and the lower part of the beam
4	R75N	ANPs and SF	75% of the perimeter surface and the lower part of the beam
5	R100N	ANPs and SF	100 % of the perimeter surface and the lower part of the beam

jack is capable of recording displacement up to 50 mm. The support distance from center to center was considered 130 cm and the distance between the two loading jaws was set at 20 cm. Loading the sample is shown in Figure 4. A displacement gauge with an accuracy of 0.01 mm was placed in the middle point of the beam to record the deformation of the mid-span at the same time as applying the load. The laboratory output diagram results show the force applied values to the beam versus the displacement values in the middle of the span. LVDT was used in the testing process, and this sensor is located just below the mid-span of the beam.

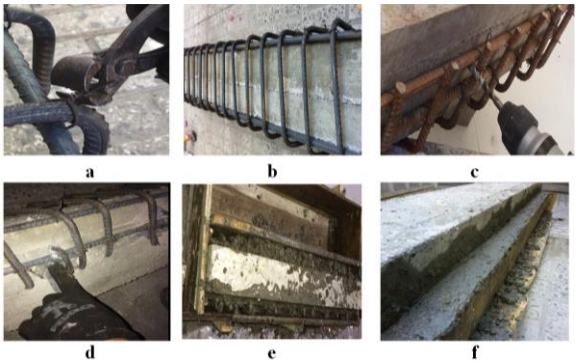

Figure 3. Steps of making and installing concrete jackets a: Making the steel reinforcement rebar b: Placing the steel rebar mesh on the beam c: Creating cavities on the surfaces of the main beams D: Installing L-shaped rebars using epoxy adhesive inside the cavities e: Concreting of jackets f: beam after concreting

Figure 4. Four-point bending flexural test

4. EXPERIMENTAL RESULTS OF RETROFITTED BEAMS

Interpretation of the beams results in the conditions with and without retrofitting was performed by examining the crack distribution and load-deflection diagrams. Crack, yield, and maximum loads as well as their corresponding deflection are considered as criteria to study the behavior of the beams. The load corresponding to the first crack is called the crack load and the displacement created in this case is called the crack deflection. The yield load is also called the load at which the steel reinforcement bars yield and the corresponding deflection is called the yield deflection. Also, the peak load is the maximum load that the beam can withstand. The deflection corresponding to the ultimate load is also defined as the ultimate deflection. According to the study conducted by Hosen et al. [43], the load-deflection curve of RC beams is divided into three distinct linear areas. The first stage is before the concrete cracks. The second stage is the cracking stage. The beam behavior at this stage is inelastic due to the creation of cracks in the cross-section and the crack expands on the peripheral surface of the beam with increasing load. The third stage is the post-cracking stage. At this stage, the concrete part is completely cracked and the steel reinforcement bars enter this stage with their strain hardness and participate in withstanding the loads.

The load-deflection curves are shown in Figure 5. Also, the failure and crack distribution of the beams at the end of loading are shown in Figure 6. In the CB beam, the first cracks were formed in the tensile region and central areas of the beam. As the load increased, the cracks extended to the beam center (near to the neutral axis) and finally, the beam failed. In the CB beam, the first crack was created in a load corresponding to 39 kN and the corresponding deflection was equal to 0.32 mm. The yield load and corresponding deflection are 99 kN and 2.4 mm, receptively.

Also, the maximum bearing load and corresponding deflection are 114 kN and 3.4 mm, receptively. The beam

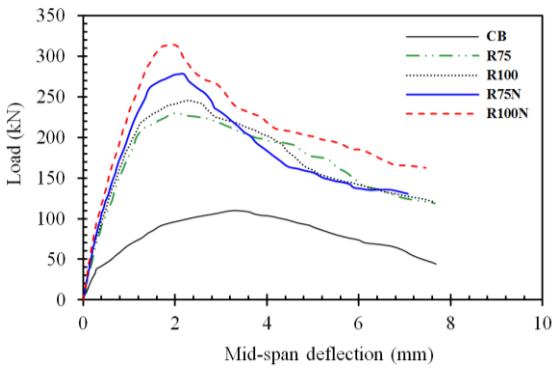

Figure 5. Comparison of the load-deflection curves (Laboratory study)

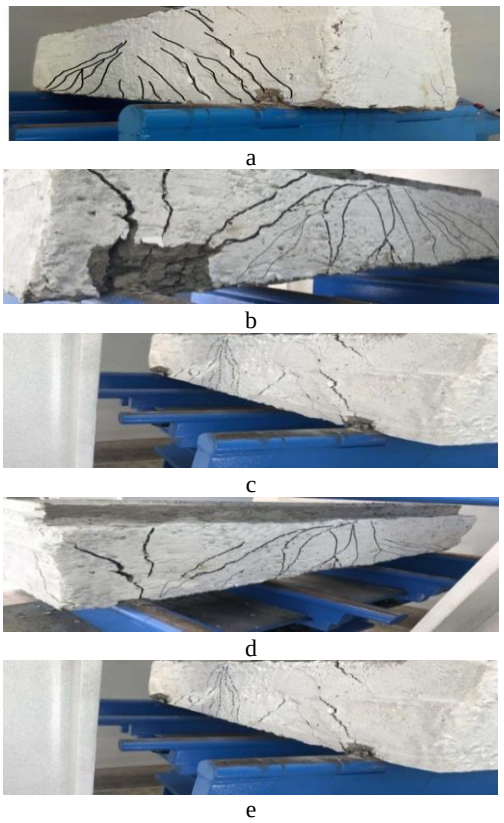

Figure 6. Beams failure and cracks distribute a: CB b: R75 c: R100 d: R75N e: R100N

ultimate displacement is 7.6 mm. In R75 beam, the crack load and crack deflection are 76 kN and 0.39 mm, respectively. The yield deflection and load are 1.21 mm and 205 kN, respectively. The maximum bearing load and the corresponding deflection are 229 kN and 1.87 mm, respectively. Also, the ultimate deflection of the beam is 7.65 mm. In R100 beam the load and crack deflection are equal to 81 kN and 0.32 mm, respectively. The yield deflection and load are 1.19 mm and 212 kN, respectively.

The beam maximum bearing load and corresponding deflection are 244 kN and 2.42 mm. Also, the beam ultimate deflection is 7.66 mm. In the R75N beam, load and crack deflection are 84 kN and 0.3 mm, respectively. Yield and load-deflection are 1.47 mm and 261 kN, respectively. The beam maximum bearing load and corresponding deflection are 277 kN and 2.19 mm, respectively. The beam ultimate deflection is 7.07 mm. In R100N beam, the crack load and displacement are 96 kN and 0.29 mm, respectively, and the yield load and deflection are 273 kN and 1.47 mm, respectively. The maximum bearing load and corresponding deflection are 314 kN and 1.9 mm, respectively. The beam ultimate deflection is 7.46 mm. The 4-point loading results that were examined in the laboratory study are presented in Table 4. This table shows the crack, yield, maximum and ultimate loads of the beams. Also, the corresponding deflection, ductility, and energy absorption capacity are calculated. The numbers in parentheses indicate the increased ratio in each of the quantities compared to the control beam specimen.

To investigate more, various comparative diagrams are presented. At the points where cracks are created, the maximum tensile stress is created in the farthest thread of the section and the concrete has lost its tensile strength. The load at which cross-sectional cracking occurs is called the "cracking load" (P_{cr}). The crack load of all the beams is presented in Figure 7. In all cases, the use of the proposed concrete jackets has increased the crack load. The crack load of the retrofitted beams with RC jackets without ANPs was 95 and 107% higher than the crack load, respectively.

The crack load of the retrofitted beams with RC jackets containing ANPs was 115 and 146% higher than the crack load, respectively. ANPs fill the cement and silica fume voids and increase the beam resistance against cracking by creating more adhesion. Concrete crushing is one of the common problems in the concrete structural elements. In this study, it has been observed that the crushing in concrete without ANPs is stronger than the concrete contains ANPs because ANPs affect the concrete matrix and reduce its crushing. Reducing the crushing of concrete by using ANPs and SF in RC beams can reduce the cost of retrofitting and maintenance after low to medium magnitude earthquakes. The yield loads of the beams are compared in Figure 7. The use of RC jackets containing ANPs has increased the yield load by about 164 to 176%, depending on the type of jacket arrangement. Also, the yield load of retrofitted beams with jackets in which normal concrete was used has increased by about 107 to 114%. According to the mentioned values, it can be stated that the use of ANPs has caused the reinforcement bars to yield later and the beams yield-bearing capacity has increased.

The maximum load of the beams is the bearing capacity of the beams. The beams bearing capacity are compared in Figure 7. The results show that the use of concrete jackets without and containing ANPs, depending on their arrangement, can increase the bearing capacity of RC beams by about 107 to 175%. Concrete jackets increase the flexural stiffness of the beams by enclosing them around the beam and increase the moment of inertia, making the beams able to withstand more loads.

As expected, in cases where the jacket covers the entire perimeter of the beams, the beam bearing capacity is greater than in cases where the jacket covers 75% of the peripheral surface. The difference between the RC beams bearing capacity with R100 jackets without and containing ANPs compared to their corresponding values in retrofitting beams with R75 jackets is 2.8 and 22.3%, respectively. This means that the change in the

TABLE 4. Comparison of the results of laboratory study and finite element study

Beam name	Crack load			Yield load			Maximum Load			Ultimate Load			Flexural toughness (J)		
	P_{cr} (kN)			P_y (kN)			P_{max} (kN)			P_u (kN)					
	EXP	FEM	Error (%)	EXP	FEM	Error (%)	EXP	FEM	Error (%)	EXP	FEM	Error (%)	EXP	FEM	Error (%)
CB	39	38	2.6	99	98	1	114	112	1.8	49	48	2	616	591	1.4
R75	76	74	2.6	205	180	12.2	229	228	0.4	119	123	3.4	1310	1271	3
R100	81	80	1.2	212	227	1.4	244	249	2	120	125	4.2	1331	1355	1.8
R75N	84	75	10.7	261	250	4.2	277	278	0.4	131	148	13	1294	1385	7
R100N	96	98	2.1	273	275	0.7	314	320	1.9	163	175	7.4	1587	1549	2.4

arrangement of jackets containing nanoparticles has a greater effect on changing the bearing capacity of the beams.

The percentage increase in the crack, yield, and maximum loads in beams retrofitted with a jacket containing ANPs compared to their corresponding values in beams retrofitted with jackets without nanoparticles are shown in Figure 8. In R75 beams, crack, yield and maximum loads have increased by 10.5, 27.3, and 21%, respectively. Also, in R100, the crack, yield, and maximum loads have increased by 18.5, 28.8 and 28.7%, respectively. The mentioned values indicate that ANPs have an effective role in improving the RC beams retrofitted with concrete jackets response. The reason for improving the bearing capacity in reinforced specimens of jackets containing ANPs compared to specimens without ANPs is that nanoparticles increase the beam resistance against incoming loads by increasing the tensile strength of concrete and inhibiting cracks produced on the concrete surface.

Energy absorption capacity or flexural strength is one of the parameters examined to analyze the reinforced concrete member's performance. The higher energy absorption capacity is shown the better member performance. The beam's energy absorption capacity was calculated by determining the area under the load-deflection curve. The energy absorption capacity of the beams is shown in Figure 9. The flexural toughness of all RC beams was increased compared to the reference beam. The energy absorption capacity of beams R75, R100, R75N, and R100N compared to the reference beam has increased by 112, 116, 110, and 157%, respectively. The use of ANPs in concrete jackets has been effective and has caused the RC beam to have a higher energy absorption capacity.

According to Figure 9, it is observed that in retrofitted beams with concrete jackets containing ANPs, more collision of beam surfaces with jacket surfaces leads to

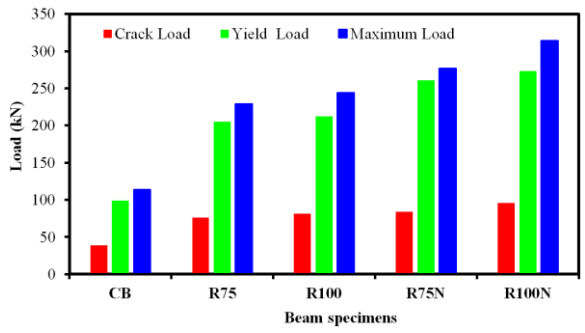

Figure 7. Comparison of crack, yield, and maximum loads

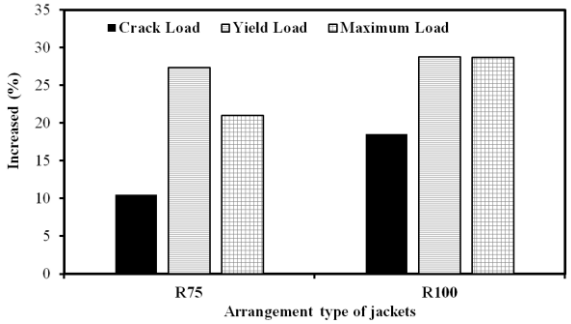

Figure 8. The percentage increase of crack, yield, and maximum loads in retrofitted beams with jackets containing ANPs compared to control beams

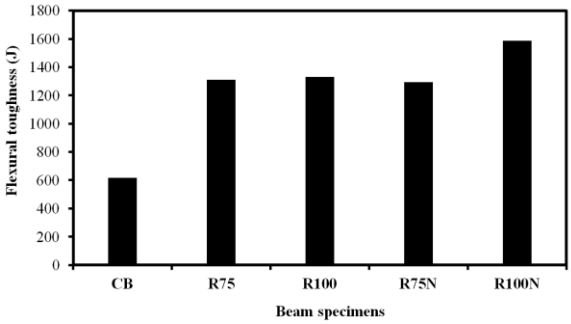

Figure 9. Comparison of flexural toughness (energy absorption capacity)

the further increase of energy absorption capacity. However, in retrofitted beams with concrete jackets without nanoparticles, the change in the type of jacket arrangement has little effect on increasing the energy absorption capacity.

Ductility capacity or ductility coefficient is defined based on the ultimate deflection ratio (Δ_u) to yield deflection (Δ_y) and is calculated using Equation (1) [11]. In Figure 10, the ductility coefficient of the studied beams was compared with each other.

$$\mu = \frac{\Delta_u}{\Delta_y} \quad (1)$$

The use of concrete jackets has caused the beams to be more ductile compared to the control beam. According to the considered variables, the beams ductility has increased by about 56 to 85%. RC jackets without nanoparticle performed much better in terms of ductility than the RC jackets containing nanoparticles; however, the nanoparticles used in the jacket have increased the yield, compressive and tensile strengths, but the deformation corresponding to the yield load is much higher compared to RC jackets without nanoparticle, which reduces the ductility. Also, Figure 10 shows that the greater the involvement of the proposed concrete jacket with the surrounding surface of the beam leads to more ductility. This is true for both jackets with and without nanoparticles; the ductility coefficient of RC beams with jackets without nanoparticles and with R100 arrangement has increased by 2 and 19%, respectively, compared to the corresponding values in RC beams with R75 arrangement.

5. FINITE ELEMENT SIMULATION

After completing the laboratory steps, RC beams retrofitted with concrete jacket containing ANPs were simulated and subjected to loading according to laboratory conditions, and their load-deflection curves were determined. After ensuring the accuracy of the method used in the simulation, which was performed using laboratory studies, variables such as the beam span length (1.5, 3, 4.5 m), the concrete jacket thickness (4, 8, and 12 cm), and the diameter of reinforcement bar used in the jacket (8, 10 and 12 mm) for retrofitting were investigated. The main beam strength is constant and equal to 21 MPa. According to the laboratory results, it was generally concluded that the use of 2.5% ANPs has a greater effect on improving the concrete mechanical properties and strength; therefore, this type of concrete characteristics have been used to simulate all concrete jackets. According to the load-deflection curves, it was concluded that when the concrete jackets are placed on 100% of the perimeter and the bottom of the beam, the response of the beam is much better than the cases where the jacket is on 75% of the perimeter and beam bottom. Therefore, the R100 model was selected in finite elements simulating the beams. The models are presented in Table 5. In this table, the letter L and the number after it represent the word length and the beam length,

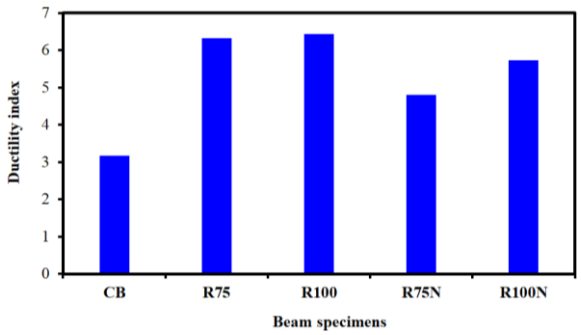

Figure 10. Comparison of ductility index

TABLE 5. Finite element models of the investigated beams

Case	Beam name	Jacket thickness (mm)	The rebar diameter used in RC Jacket	Beam span (mm)
1	L1.5	----	----	1500
2	L1.5-d8-t4	4	8	
3	L1.5-d8-t8	8		
4	L1.5-d8-t12	12		
5	L1.5-d10-t4	4	10	
6	L1.5-d10-t8	8		
7	L1.5-d10-t12	12		
8	L1.5-d12-t4	4	12	
9	L1.5-d12-t8	8		
10	L1.5-d12-t12	12		
11	L3	----	----	3000
12	L3-d8-t4	4	8	
13	L3-d8-t8	8		
14	L3-d8-t12	12		
15	L3-d10-t4	4	10	
16	L3-d10-t8	8		
17	L3-d10-t12	12		
18	L3-d12-t4	4	12	
19	L3-d12-t8	8		
20	L3-d12-t12	12		
21	L4.5	----	----	4500
22	L4.5-d8-t4	4	8	
23	L4.5-d8-t8	8		
24	L4.5-d8-t12	12		
25	L4.5-d10-t4	4	10	
26	L4.5-d10-t8	8		
27	L4.5-d10-t12	12		
28	L4.5-d12-t4	4	12	
29	L4.5-d12-t8	8		
30	L4.5-d12-t12	12		

respectively. The letter d indicates the diameter and the number after it is the diameter of the reinforcement bars used in the jacket. The letter t and the number after representing the thickness and the jacket thickness. For example, the term L1.5-d10-t12 describes a condition in which a 1.5 m long concrete beam is retrofitted by a 12 mm thickness concrete jacket and the reinforcement bars diameter used in the jacket is 10 mm. The desired outputs include damage distribution and load-deflection curve, respectively. The results are interpreted using load-deflection curves and energy absorption capacity. The effect of each studied variables and determining the most optimal states has been done by calculating the area under the load-deflection curve (energy absorption capacity), crack, yield and maximum loads and the corresponding deflections as well as ductility. The geometric and reinforcement bars characteristics of the main beams are shown in Figure 11.

The beam length and dimensions are 1500 mm and 150×200 mm, respectively. Two reinforcement bars with a diameter of 12 mm at the bottom of the beam and two reinforcement bars with a diameter of 12 mm at the top of the beam were used. Also, the shear reinforcement bars diameter was 10 mm, and their space was considered about 200 mm apart. The support conditions and how the load is applied to the beams models are shown in Figure 12. In all cases, mid-span deflection and the corresponding load are extracted as output. A schematic image of retrofitted beams is shown in Figure 13. They used reinforcement bar mesh in the jacket consists of a reinforcement bar with a diameter of 10 mm. The spaces between reinforcement bars were considered 50 mm. Finite element analysis of RC beams was performed using ABAQUS software [41].

ABAQUS can simulate numerical models of concrete for the nonlinear response. The model's dimensions are similar to the tested beams in the laboratory program. The simulation structural elements include beam rectangular cross-section, U-section jacket, the longitudinal reinforcement bars used in the beam, the transverse

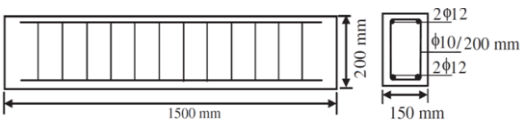

Figure 11. Geometric specifications and steel reinforcement details of beams (FEM beams)

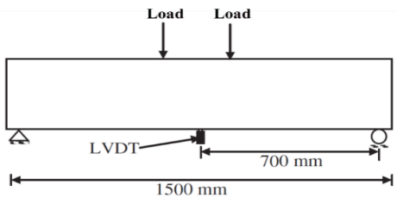

Figure 12. Support conditions of the beams

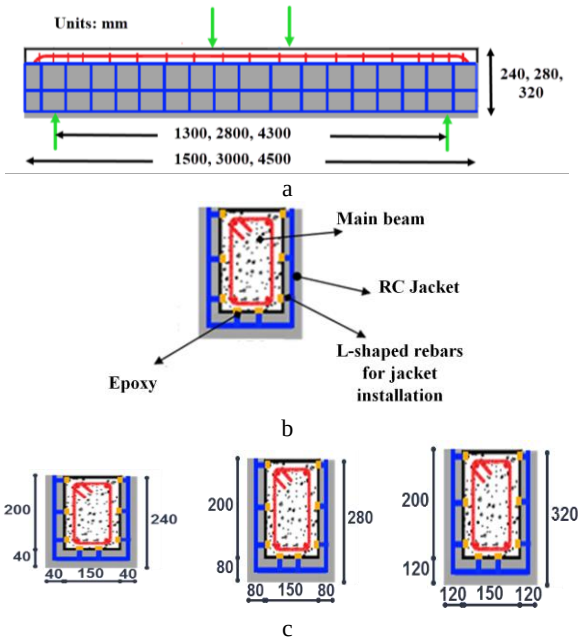

Figure 13. Schematic of retrofitted beams a: Overview of the RC beams b: Different parts of RC jacket c: The sections of retrofitted beams

reinforcement bars (stirrup) used in the beam, and the jacket reinforcement bar mesh. These elements are deformable. The solid element was used to simulate concrete and the wire element was used to simulate reinforcement bars. The C3D8R element was used to simulate the concrete.

The stress-strain ideal elastic-plastic curve of reinforcement bars are applied by measuring the yield stress values. The materials behavior provided with ABAQUS (using PLASTIC settings) allows the use of a nonlinear stress-strain curve. The Von Mises yield criterion is used to define the yield isotropic of steel materials. The compressive strength of the main beam concrete was 21 MPa. Compressive and tensile strengths of the concrete used in the jacket were considered 49.14 and 3.4 MPa, respectively. According to Table 2, the concrete used in the jacket is the same as NA2.5 concrete, in which 2.5% of ANPs are used in combination with cement and SF. Based on results of the reinforcement bar tensile test, yield stress and reinforcement bars elasticity modulus is 200 (GPa) and 420 MPa, respectively. The materials used specifications are presented in Table 6. The interaction between steel reinforcement bras and concrete was defined using the embedded method. The meshing step is one of the most important steps in finite element simulations. In finite element problems, the optimal meshing method should be used, to achieve appropriate responses. For this purpose, the stress created at a specific point of the beams was considered and in the next step, the elements were doubled (the element's dimensions were halved) and the model was analyzed

TABLE 6. Specifications of materials defined in the finite element models

	f_c (MPa)	f_t (MPa)	υ
Concrete of the main beams	21	2.9	0.2
Concrete of the RC jacket	49.14	3.4	
	E_s (GPa)	**f_y (MPa)**	υ
Steel reinforcement rebar	200	420	0.3

again to measure the effect of this fine-tuning on the stress. This must continue until a compromise between time and the number of elements; In other words, by increasing the number of the elements, there is no significant change in the obtained response. In such a case, it can be said that the responses are converged, and increasing the number of the elements has no effect on increasing the accuracy of the response. The sweep technique was used for meshing. This method is suitable for modeling with complex surfaces. The concrete behavior is defined using concrete damaged plasticity. This model is based on the hypothesis of isotropic damage and is designed for situations where the concrete is under arbitrary loads. This model considers the effect of stiffness recovery as the result of a plastic strain, both in tension and in pressure. In RC, the post-failure behavior properties are generally determined by giving the fracture stress as a function of the crack $\tilde{\varepsilon}_t^{cr}$. Crack strain is the total strain minus the elastic strain corresponding to the non-damaged material (Equations (2) and (3)).

$$\varepsilon_c^{in} = \varepsilon_c - \varepsilon_c^{el} \tag{2}$$

$$\varepsilon_c^{in} = \frac{\sigma_c}{E_0} \tag{3}$$

$$\varepsilon_c^{\sim pl} = \varepsilon_c^{\sim in} - \frac{d_c}{(1-d_c)}\frac{\sigma_c}{E_0} \tag{4}$$

Tensile stiffening data are entered by the crack strain. When loading data is available, the data is prepared to be given as a tensile damage curve to the ABAQUS program [41]. The program automatically converts the cracking strain values to the plastic strain values using Equations (6) and (7) (Figure 14).

$$\varepsilon_t^{cr} = \varepsilon_t - \varepsilon_t^{el} \tag{5}$$

$$\varepsilon_t^{el} = \frac{\sigma_t}{E_0} \tag{6}$$

$$\varepsilon_t^{\sim pl} = \varepsilon_t^{\sim ck} - \frac{d_t}{(1-d_t)}\frac{\sigma_t}{E_0} \tag{7}$$

The compressive inelastic strain is the total strain minus the elastic strain corresponding to the material being damaged. The program automatically converts the inelastic strain values into plastic strain values using the following illustration (Figure 15).

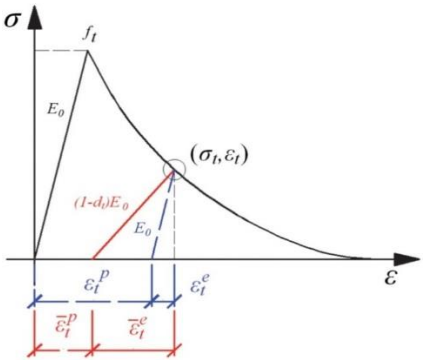

Figure 14. Cracking strain used to define tensile stiffness data [41]

6. VALIDATION

In numerical and software simulations, performing the validation process is one of the steps that lead to ensuring the analysis results. In the present study, the accuracy of the method and behavioral models used in the modeling of RC beams was evaluated and the results are presented in this section. All of the five beams were simulated using the methods and behavioral models presented in section 5 and the load-deflection and crack distribution (failure) diagrams are presented in Figures 16 and 17. Figures 16-a and 17-a compare the CB laboratory results and the finite element analysis. The failure range and the cracks created in the finite element model (FEM) and the experimental (Exp.) specimen are very close to each other. The crack angle created relative to the horizon is about 45 degrees and most of the cracks are created in the area between the support and the span center.

The crack, yield, maximum and ultimate loads of the FEM of CB are 38, 98, 112, and 48 kN, respectively, and the crack, yield, maximum and ultimate loads of the experimental specimen of the control beam are 39, 99,

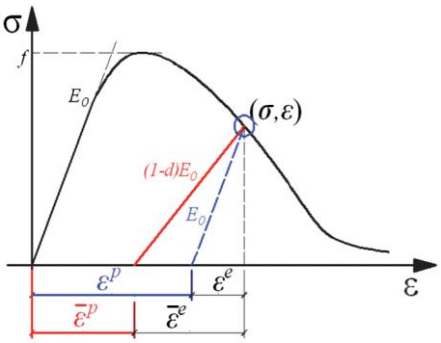

Figure 15. Inelastic compressive strain to define compressive stiffness data [41]

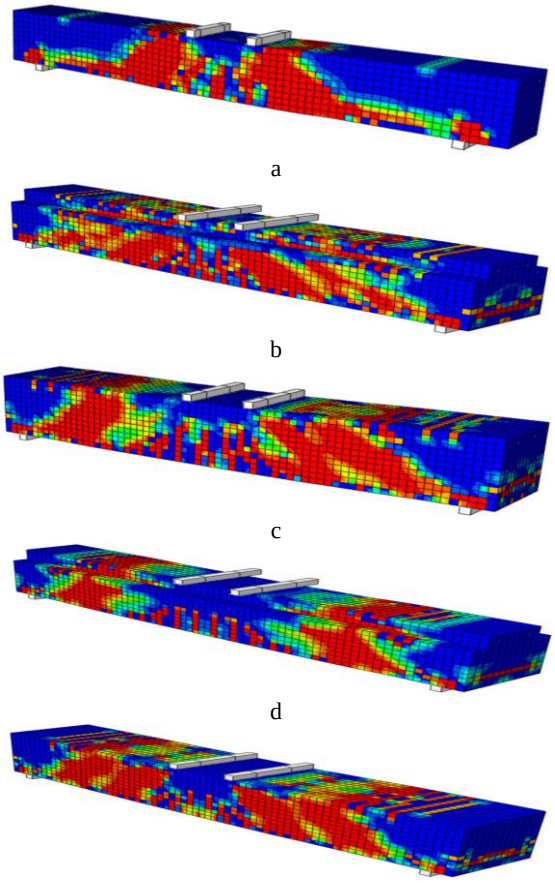

Figure 16. Damage distribution of FEMs of beams a: CB b: R75 c: R100 d: R75N e: R100N

114 and 49 kN, respectively. The difference between crack, yield, maximum and ultimate loads of FEM and Exp. of CB is 2.6, 1, 1.8, and 2%, respectively. The energy absorption capacity of FEM and Exp. of CB beam are 616 and 591, respectively and the difference between them is about 4%.

The FEM and Exp. specimen of R75 are presented in Figures 16-a and 20-b. According to the load-deflection curve, the difference between crack, yield, maximum and ultimate loads is 2.6, 12.2, 0.4, and 3.4%, respectively. Also, the energy absorption capacity of FEM and Exp. specimen of R75 is equal to 1310 and 1271 kJ, respectively and the difference between them is about 3%.

The failure distribution and load-deflection curve of FEM and Exp. specimen of R100 are presented in Figures 16-a and 17-c. This beam is retrofitted using concrete jacket without nanoparticles. These jackets were covered 100% of the beams perimeter. According to the load-deflection curve, crack, yield, maximum and ultimate loads of R100 FEM are 80, 227, 249, 125 kN, respectively. Also, the crack, yield, maximum and ultimate loads of R100 Exp. specimen are 81, 212, 244, 120 kN, respectively and the difference between them is 1.2, 1.4, 2, and 4.2 percent, respectively. Also, the energy absorption capacity of FEM and Exp. Specimen of R100 is equal to 1355 and 1331 kJ, respectively and the difference between them is about 1.8%. The crack pattern distribution in both FEM and Exp. specimen is very close to each other; in both cases, cracks have been created in the area between the center and the supports.

The failure distribution and load-deflection curves of the R75N beam obtained from FEM analysis and laboratory study are shown in Figures 16-b and 17-d. This beam is retrofitted with concrete jacket containing ANPs and SF. These jackets cover 75% of the beams perimeter. According to the load-deflection curve, the crack, yield, maximum and ultimate loads of the R75N FEM are 75, 250, 278, and 148 kN, respectively. Also, the crack, yield, maximum and ultimate loads of the R75N beam laboratory sample are 84, 261, 277, and 131 kN, respectively. The difference between the values of crack, yield, maximum and ultimate loads of the FEM and Exp. specimen of R75N is 10.7, 4.2, 0.4, and 13%, respectively. Also, the energy absorption capacity obtained from finite element analysis and laboratory study of R75N beam is 1385 and 1294 kJ, respectively.

The finite element analysis and laboratory study results of the R100N beam are shown in Figures 16-b and 17-e. This beam is retrofitted with concrete jacket containing ANPs and SF, and the concrete jacket covers

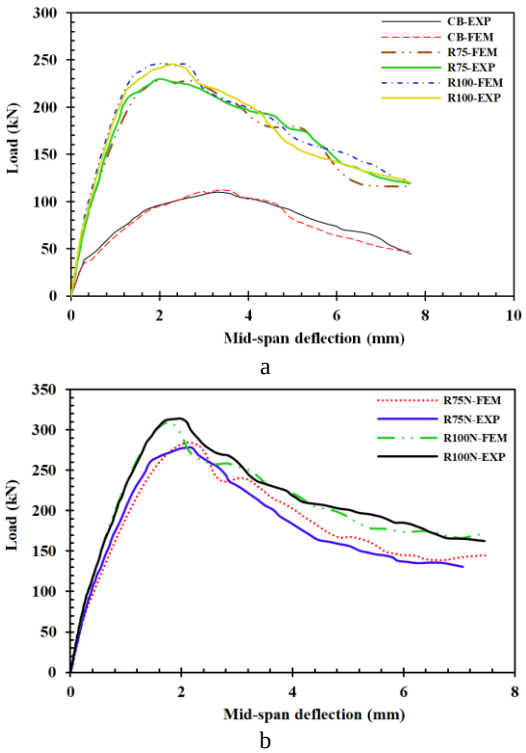

Figure 17. Load-deflection curves of the beams a: CB, R75, and R100 b: R75N and R100N

all sides and bottom of the beam. According to the load-deflection curves, the crack, yield and maximum, and ultimate loads of R100N FEM are 98, 275, 320, and 175 kN, respectively. Also, the crack, yield, maximum and ultimate loads of R100N Exp. specimen are 96, 273, 314 and 163 kN, respectively. The difference between crack, yield, maximum and ultimate loads obtained from the FEM and laboratory study are 2.1, 0.7, 1.9, and 7.4%, respectively. Crack distribution of R100N beam shows that the use of ANPs affects reducing crack distribution in beams.

Energy absorption capacity, crack, yield, maximum and ultimate loads are presented in Table 7. In this table, the percentage difference of load values obtained from finite element analysis (FEM) to the corresponding values in the laboratory study (EXP) is obtained. The difference of crack load, yield load, maximum load, ultimate load and, energy absorption capacity is about 2.1 to 10.7%, 0.7 to 12.2 %,.4 to 1.9%, 2 to 13 %, and 1.4 to 7%, respectively. According to the load-deflection curves and the comparison of laboratory specimens and numerical models simulated by ABAQUS software, it is observed that the maximum load and deflection values of experimental specimens and finite elements are close to each other; therefore, the results of the method used in this study, which is performed using ABAQUS software, have a relatively good agreement with the laboratory results.

7. FINITE ELEMENT ANALYSIS RESULTS

7. 1. Energy Absorption Capacity The flexural strength (energy absorption capacity) and its percentage increase compared to the control beams are shown in Figure 18. The use of reinforcement concrete jacket containing ANPs, depending on the jacket thickness, the number of reinforcement bars used in the jacket, and the length of the beam span, increased the flexural strength of the beams about 2.55 to 5.55 times compared to control specimens. The increase of flexural strength in beams retrofitted with RC jacket containing ANPs that have longer spans is much higher than beams with shorter spans. For example, the increase in flexural strength of the L4.5-d12-t12 beam is 5.47 times compared to the control specimen; this is while the increase in flexural strength of the L1.5-d12-t12 beam is 4.94 times compared to the control specimen.

The effect of changes in the thickness and diameter of the jacket of the reinforcement bars used in the jacket on

TABLE 7. Comparing the results of laboratory and finite element study

Beam name	Crack load			Yield load			Maximum Load			Ultimate Load			Flexural toughness (J)		
	P_{cr} (kN)			P_y (kN)			P_{max} (kN)			P_u (kN)					
	EXP	FEM	Error (%)	EXP	FEM	Error (%)	EXP	FEM	Error (%)	EXP	FEM	Error (%)	EXP	FEM	Error (%)
CB	39	38	2.6	99	98	1	114	112	1.8	49	48	2	616	591	1.4
R75	76	74	2.6	205	180	12.2	229	228	0.4	119	123	3.4	1310	1271	3
R100	81	80	1.2	212	227	1.4	244	249	2	120	125	4.2	1331	1355	1.8
R75N	84	75	10.7	261	250	4.2	277	278	0.4	131	148	13	1294	1385	7
R100N	96	98	2.1	273	275	0.7	314	320	1.9	163	175	7.4	1587	1549	2.4

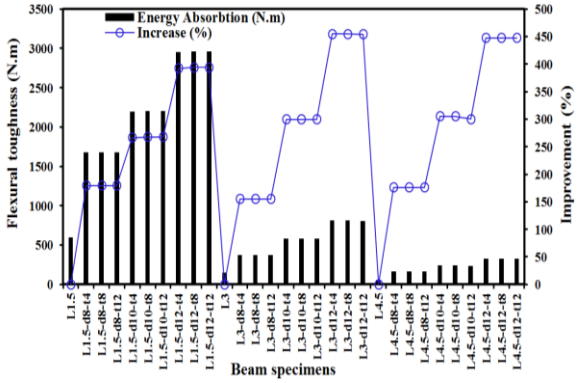

Figure 18. Comparison of flexural strength (energy absorption capacity) of the finite element model of the beams

the flexural strength of RC beams with 1.5, 3, and 4.5 meters length is investigated in Figure 19. The reinforcement bars area used in concrete jacket containing ANPs has a significant effect on increasing the beams flexural strength. Thus, in beams with lengths of 1.5, 3, and 4.5 meters, increasing the steel reinforcement bars diameter to 1.5 times increased the flexural strength of the beams by 76, 117 and 98%, respectively. According to Figures 19-b and 19-c, increasing the thickness of the concrete jacket has little effect on increasing the beams flexural strength, and only in a few beams, the flexural strength increased. Therefore, in terms of flexural strength and economic issues, the use of RC jackets containing ANPs with less thickness is a better option; because increasing the

thickness has little effect on improving the flexural strength result.

The bearing capacity of retrofitted beams with RC jackets containing ANPs did not change significantly due to the change in jacket thickness. Increasing the jacket thickness had little effect on increasing the beams bearing capacity. Increasing the diameter of jackets reinforcement bars from 8 mm to 12 mm for all three beam types with different lengths had a significant effect on increasing the beams bearing capacity. The flexural strength of retrofitted beams with 1.5 m length, which reinforcement bars with 10 and 12 mm diameter were used in jackets, were increased 29 and 85%, respectively, compared to the retrofitted beams with 8 mm rebar in jackets. The energy absorption capacity of the beams with a length of 4.5 meters, in which RC jackets with 10 and 12 mm rebar were used increased by 90 and 34%, respectively, compared to jackets with 8 mm bars.

7. 2. The Maximum Bearing Load The bearing capacity (section resistance moment) and the increase ratio compared to the control beams are presented in Figure 20. The proposed retrofitting method increased the bearing capacity of the beams with a length of 1.5, 3, and 4.5 m about 2.87 to 5.05 times, 2.31 to 4.55, and 2.38 to 4.57 times, respectively.

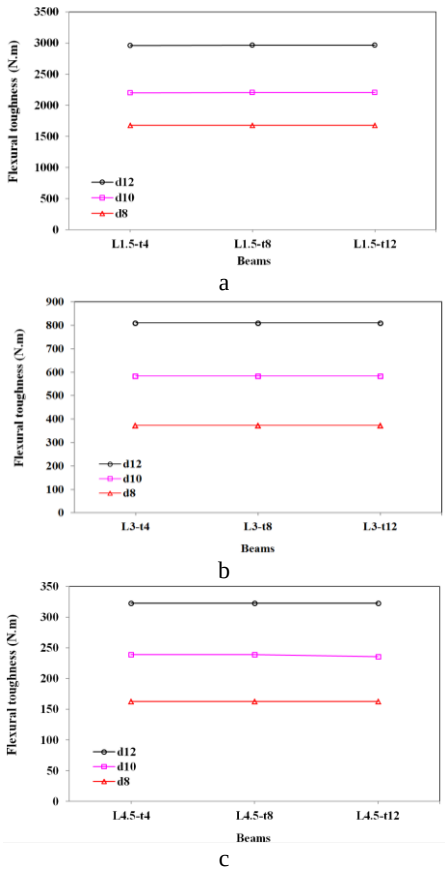

Figure 19. Investigation of the effect of changing the jackets thickness and the diameter of the rebars used in the jackets on the flexural toughness of the beams a: 1.5 meters beam b: 3 meters beam c: 4.5 meters beam

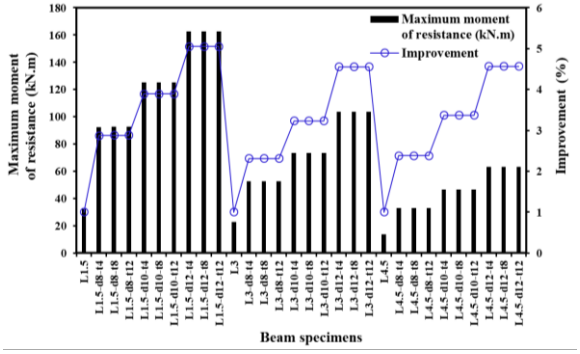

Figure 20. Comparison of the bearing capacity (section resistance moment)

7. 3. Yield Load The yield loads of the thirty beams and their increased values relative to the reference beams are shown in Figure 21. The use of RC jacket containing ANPs has increased the yield load of 1.5, 3, and 4.5 meters beams depending on the diameter of the jacket reinforcement bars and the thickness of the jacket about 2.96 to 5.43, 2.29 to 4.4, and 2.09 to 3.93 times, respectively. According to Figure 21, the percentage of yield load has increased in beams with smaller spans. With increasing the span length, the effect of the proposed method on the increase percentage of yield load has decreased. As changes in the energy absorption capacity and bearing capacity obtained, the yield load of the reinforced beams under study does not change significantly due to changes in the jacket thickness. The percentage of steel used in concrete jackets has an effect on improving the yield load. For example, in 1.5, 3 and 4.5 meters beams that have been retrofitted by concrete jackets containing 12 mm diameter rebars, the yield load is approximately 84, 92 and 83% more than the 1.5, 3 and 4.5 m beams which reinforced with 8 mm diameter rebars.

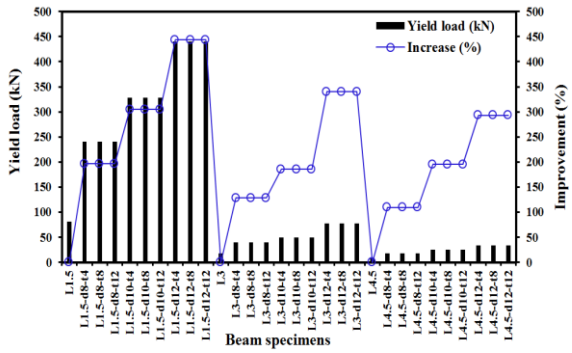

Figure 21. Comparison of the yield load of the examined beams

7. 4. Crack Load The crack loads of the FEM beams is presented in Figure 22. In all cases, the crack load of the retrofitted beams is increased. The proposed concrete jacket has been able to increase the crack load of 1.5, 3 and 4.5 meters beams by 2.03 to 5 times, 3.5 to 7.25 times, and 1.38 to 3.45 times, respectively.

Figures 23 to 25 investigate the effect of changes in the thickness of the jackets and the diameter of the jackets rebars on the percentage of increase in the crack load of beams with a length of 1.5, 3, and 4.5 meters. As can be seen, increasing the thickness of concrete jackets in beams with a span of 1.5 meters has been effective and has been able to increase the resistance of the beam to cracking. For example, the crack load of the L1.5-d12-t12 beam has increased 4 times (400%) compared to the reference beam; This is while the L1.5-d12-t4 beam is 130% more than the reference beam. As the length of the beam increases, the thickness does not play a significant role in improving the crack load (Figures 24 and 25).

Increasing the thickness of concrete jackets in beams with a span of 1.5 meters is effective and has been able to increase the crack load. For example, the crack load of the L1.5-d12-t12 beam has increased 4 times (400%) compared to the reference beam; However, the L1.5-d12-t4 beam is 130% larger than the reference beam. As the length of the beam increases, the thickness does not play a significant role in improving the crack load (Figures 27 and 28).

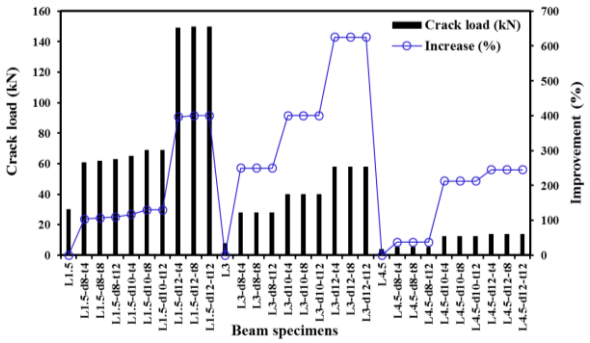

Figure 22. Comparison of the crack load of beams understudy

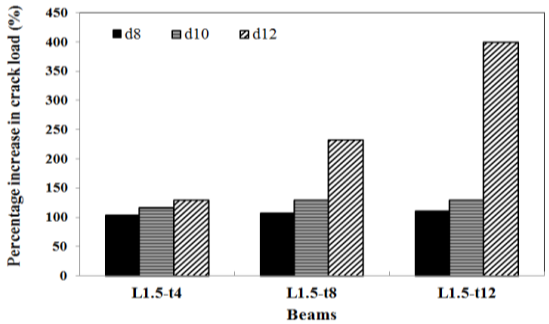

Figure 23. Investigation of the effect of change in the jacket thickness and the diameter of the rebars used in the jacket on the percentage of increase in crack load (1.5-meter beam**)**

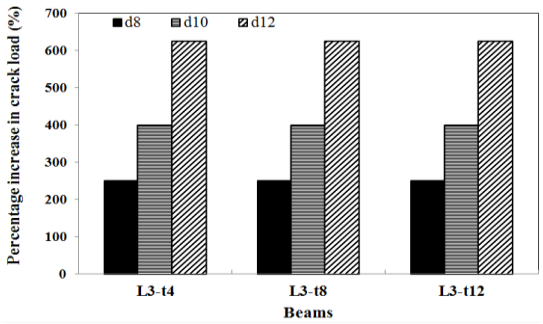

Figure 24. Investigation of the effect of change in the jacket thickness and the diameter of the rebars used in the jacket on the percentage of increase in crack load (3-meter beam**)**

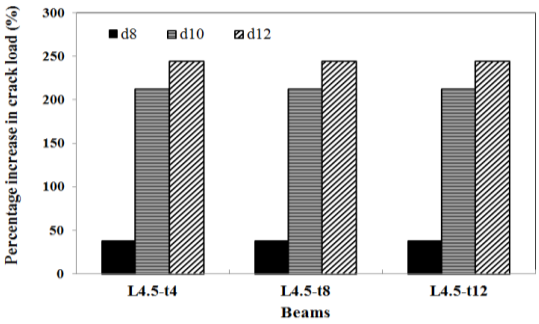

Figure 25. Investigation of the effect of change in the jacket thickness and the diameter of the rebars used in the jacket on the percentage of increase in crack load (4.5-meter beam**)**

7. 5. Comparison of Crack, Yield, and Ultimate Deflections The values of crack, yield, and ultimate deflections of the beams are presented in Figures 26-28.

The use of concrete jackets containing ANPs has a little role in the ultimate deformation of the beams and no significant difference is observed between the ultimate deflection of the beams. Concrete jackets reduced crack and yield deformations. The crack deflection of retrofitted beams with lengths of 1.5, 3, and 4.5 meters was reduced approximately between 55 to 65, 65 to 75, and 256 to 520%, respectively.

The yield deflection of the beams with concrete jackets containing ANPs is reduced in all cases compared

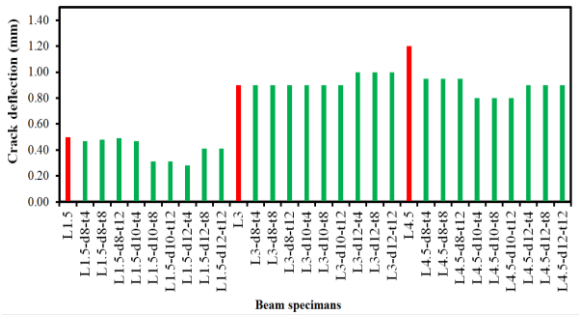

Figure 26. Comparison of crack deflections

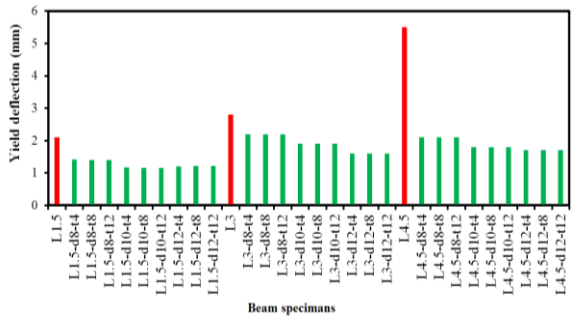

Figure 27. Comparison of yield deflections

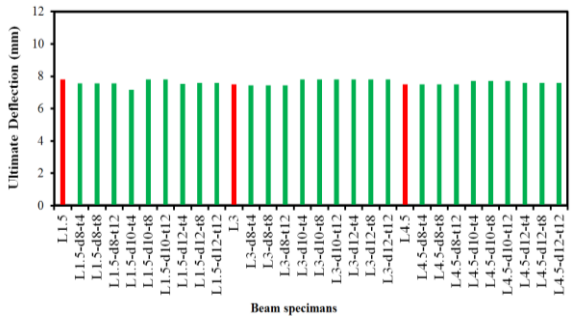

Figure 28. Comparison of ultimate deflections

to control beams. This percentage reduction is much higher in longer beams. The yield deflection of the retrofitted beams with concrete jackets containing ANPs is reduced in all cases compared to control beams.

7. 6. Ductility Capacity The ductility factor of the beams is presented in Figure 29. Concrete jackets containing ANPs have increased the ductility of 1.5 meters of concrete beams by 1.44 to 1.81 times, depending on the thickness and diameter of the rebars. Also, the ductility coefficient of retrofitted beams with a span length of 3 meters has increased approximately 1.26 to 1.82 times. The ductility coefficient of retrofitted beams with a span length of 4.5 meters has increased approximately 2.63 to 3.29 times compared to the reference beam.

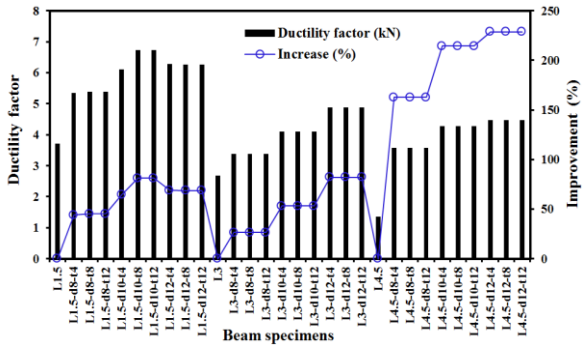

Figure 29. Comparison of ductility factor

8. SUMMARY AND CONCLUSIONS

In this paper, laboratory and numerical investigation of RC beams were performed using RC jackets with SCC containing ANPs and SF. The laboratory study was performed in two stages. In the first stage, the properties of hardened concrete (compressive, tensile, and flexural strengths, water absorption) and the properties of fresh concrete (slump flow, T50, funnel V, box L) of SCC containing ANPs were investigated. In the next step, several beams were made and were retrofitted using the proposed concrete jackets. ANPs were used in 13 different mixing schemes (0 to 3% by weight of cement). Also, the amount of SF in all specimens was considered constant. After examining the characteristics of fresh and hardened concretes containing ANPs and determining the most optimal design (according to the experiments), the retrofitting of RC beams using RC jackets with SCC jackets containing ANPs was investigated. For this purpose, 1.4 metes RC beams with the same dimensions and specifications of steel reinforcement were made and subjected to four-point loading in the conditions with and without retrofitting. Ordinary concrete was used in the concrete jacket once and ANPs (the most optimal design) were used again.

Concrete jackets once covered all of the perimeter and bottom surfaces of the beams and again 75% of the perimeter and bottom surfaces. After completing the laboratory steps, RC beams were simulated according to laboratory conditions using FEM and ABAQUS software. A parametric study was performed and parameters such as beam length (1.5, 3, 4.5 m), concrete jacket thickness (4, 8, and 12 cm), and the diameter of rebars used in the jacket (8, 10, and 12 mm) was examined. The most important results are presented following:

- The addition of ANPs reduced the pore size of the concrete specimens and makes them denser. This can be due to the effects of nanoparticle filling, pozzolanic properties as well as swelling of ANPs.
- Crushing of concrete is one of the common problems in the elements of concrete structures. In this study, it has been observed that the concrete crushing without nanoparticles is more than the concrete contain nanoparticles. Because nanoparticles affect the concrete matrix and reduce its crushing. Reducing the brittleness of concrete by using ANPs and silica fume in RC beams can reduce the cost of reinforcement and maintenance after low to medium magnitude earthquakes.
- The use of RC jackets containing ANPs has increased the yield load by about 164 to 176%, depending on the arrangement of the jacket. Also, the yield load of beams that are not coated with nanoparticles has increased by about 107 to 114%.
- The results show that the use of concrete jackets without and containing nanoparticles, depending on the

arrangement they have, can increase the bearing capacity of reinforced concrete beams by about 107 to 175 percent. Concrete jackets increase the flexural stiffness of the beams by enclosing them around the beam and increasing the moment of inertia of the beam, making the beams able to withstand more loads.

- The flexural strength of all reinforced beams is increased compared to the reference beam. So that the energy absorption capacity of each of the beams R75, R100, R75N, and R100N compared to the reference beam has increased by 112, 116, 110, and 157 %, respectively. The use of nanoparticles in concrete jackets has been effective and has caused the RC beam to have a higher energy absorption capacity.
- In retrofitted beams with a concrete jacket containing ANPs, the more surfaces of the beam are involved with the jacket, the more energy absorption capacity will be. However, in retrofitted beams with concrete jackets without nanoparticles, the change in the type of jacket arrangement has little effect on increasing the energy absorption capacity.
- The use of concrete jackets has caused the behavior of the beams to be more ductile compared to the control beam. The ductility of the beams has increased by about 56 to 85%.
- The area of rebars used in concrete jackets containing ANPs has a significant effect on increasing the flexural strength of beams; Thus, in beams with lengths of 1.5, 3, and 4.5 meters, increasing the diameter of the steel rebar to 1.5 times increased the flexural strength of the beams by 76, 117 and 98%, respectively.
- In terms of flexural strength and economic issues, the use of RC jackets containing nanoparticles with a smaller thickness is a desire option. Because increasing the thickness has little effect on improving the resulting flexural strength.
- The area of rebars used in concrete jackets containing ANPs has a significant effect on increasing the flexural strength of beams. Thus, in beams with lengths of 1.5, 3, and 4.5 meters, increasing the diameter of the steel rebar to 1.5 times, increased the flexural strength of the beams by 76, 117 and 98%, respectively.

According to the results of the present study, the use of ANPs in RC jackets to retrofit RC beams is considered as a suitable solution to increase the bearing capacity. However, retrofitting of beams with this method can depend on several factors. Therefore, to develop the present study, the following suggestions are presented:

- Investigating the effect of dynamic loads on the beams retrofitted with RC jackets containing ANPs.
- Investigating the movement (slip) of the jackets containing nanoparticles on the surface of the old concrete beam.
- Investigating the use of other nanoparticles such as silica oxide nanoparticles and clay nanoparticles in RC jackets for retrofitting of concrete beams.

9. REFERENCES

1. Osman, B. H., Wu, E., Ji, B., and S Abdelgader, A. M., "A state of the art review on reinforced concrete beams with openings retrofitted with FRP", ***International Journal of Advanced Structural Engineering***, Vol. 8, No. 3, (2016), 253–267. doi:10.1007/s40091-016-0128-7
2. Negro, P., and Mola, E., "A performance based approach for the seismic assessment and rehabilitation of existing RC buildings", ***Bulletin of Earthquake Engineering***, Vol. 15, No. 8, (2017), 3349–3364. doi:10.1007/s10518-015-9845-8
3. Seifi, A., Hosseini, A., Marefat, M. S., and Zareian, M. S., "Improving seismic performance of old-type RC frames using NSM technique and FRP jackets", ***Engineering Structures***, Vol. 147, (2017), 705–723. doi:10.1016/j.engstruct.2017.06.034
4. Durgadevi, S., Karthikeyan, S., Lavanya, N., and Kavitha, C., "A review on retrofitting of reinforced concrete elements using FRP", ***Materials Today: Proceedings***, (In Press), (2020). doi:10.1016/j.matpr.2020.03.148
5. Jose, J., Nagarajan, P., and Remanan, M., "Utilisation of Ultra-High Performance Fiber Reinforced Concrete(UHPFRC) for Retroffiting – a Review", ***IOP Conference Series: Materials Science and Engineering***, Vol. 936, No. 1, (2020), 012033. doi:10.1088/1757-899X/936/1/012033
6. Kafi, M. A., Kheyroddin, A., and Omrani, R., "New Steel Divergent Braced Frame Systems for Strengthening of Reinforced Concrete Frames", ***International Journal of Engineering, Transaction A: Basics***, Vol. 33, No. 10, (2020), 1886–1896. doi:10.5829/ije.2020.33.10a.07
7. Jahangir, H., and Bagheri, M., "Evaluation of Seismic Response of Concrete Structures Reinforced by Shape Memory Alloys (Technical Note)", ***International Journal of Engineering, Transaction C: Aspects***, Vol. 33, No. 3, (2020), 410–418. doi:10.5829/ije.2020.33.03c.05
8. Zhu, Y., Zhang, Y., Hussein, H. H., and Chen, G., "Flexural strengthening of reinforced concrete beams or slabs using ultra-high performance concrete (UHPC): A state of the art review", ***Engineering Structures***, Vol. 205, (2020), 110035. doi:10.1016/j.engstruct.2019.110035
9. Tawfik, T. A., Aly Metwally, K., EL-Beshlawy, S. A., Al Saffar, D. M., Tayeh, B. A., and Soltan Hassan, H., "Exploitation of the nanowaste ceramic incorporated with nano silica to improve concrete properties", ***Journal of King Saud University - Engineering Sciences***, (In Press), (2020). doi:10.1016/j.jksues.2020.06.007
10. Sangi, M., Vasegh Amiri, J., Abdollahzadeh, G., and Dehestani, M., "Experimental study on fracture behavior of notched self-consolidating concrete beam strengthened with off-axis CFRP sheet", ***Structural Concrete***, Vol. 20, No. 6, (2019), 2122–2137. doi:10.1002/suco.201800204
11. Shadmand, M., Hedayatnasab, A., and Kohnehpooshi, O., "Retrofitting of Reinforced Concrete Beams with Steel Fiber Reinforced Composite Jackets", ***International Journal of Engineering, Transaction B: Applications***, Vol. 33, No. 5, (2020), 770–783. doi:10.5829/ije.2020.33.05b.08
12. Rahmani, I., Maleki, A., and Lotfollahi-Yaghin, M. A., "A Laboratory Study on the Flexural and Shear Behavior of RC Beams Retrofitted with Steel Fiber-Reinforced Self-compacting Concrete Jacket", ***Iranian Journal of Science and Technology, Transactions of Civil Engineering***, (2020), 1–17. doi:10.1007/s40996-020-00547-x
13. Trang, G. T. T., Linh, N. H., Linh, N. T. T., and Kien, P. H., "The Study of Dynamics Heterogeneity in SiO2 Liquid", ***HighTech and Innovation Journal***, Vol. 1, No. 1, (2020), 1–7. doi:10.28991/HIJ-2020-01-01-01

14. Pinheiro, A. P., "Architectural Rehabilitation and Sustainability of Green Buildings in Historic Preservation", ***HighTech and Innovation Journal***, Vol. 1, No. 4, (2020), 172–178. doi:10.28991/HIJ-2020-01-04-04
15. Das, K., Sen, S., and Biswas, P., "A Review Paper – on the Use of Nanotechnology in Construction Industry", Proceedings of Industry Interactive Innovations in Science, Engineering & Technology (I3SET2K19), (2020), 1–3. doi:10.2139/ssrn.3526716
16. Qasim, O. A., and Al-Ani, S. A., "Effect of nano-silica silica fume and steel fiber on the mechanical properties of concrete at different ages", AIP Conference Proceedings, Vol. 2213, No. 1, (2020), 020198. doi:10.1063/5.0000209
17. Shaiksha Vali, K., Murugan, B. S., Reddy, S. K., and Noroozinejad Farsangi, E., "Eco-friendly Hybrid Concrete Using Pozzolanic Binder and Glass Fibers", ***International Journal of Engineering, Transactions A: Basics***, Vol. 33, No. 7, (2020), 1183–1191. doi:10.5829/ije.2020.33.07a.03
18. Ghanbari, M., Kohnehpooshi, O., and Tohidi, M., "Experimental Study of the Combined Use of Fiber and Nano Silica Particles on the Properties of Lightweight Self Compacting Concrete", ***International Journal of Engineering, Transaction B: Applications***, Vol. 33, No. 8, (2020), 1499–1511. doi:10.5829/ije.2020.33.08b.08
19. Potapov, V., Efimenko, Y., Fediuk, R., and Gorev, D., "Effect of hydrothermal nanosilica on the performances of cement concrete", ***Construction and Building Materials***, Vol. 269, (2021), 121307. doi:10.1016/j.conbuildmat.2020.121307
20. Nazari, A., and Riahi, S., "Microstructural, thermal, physical and mechanical behavior of the self compacting concrete containing SiO2 nanoparticles", ***Materials Science and Engineering: A***, Vol. 527, Nos. 29–30, (2010), 7663–7672. doi:10.1016/j.msea.2010.08.095
21. Nazari, A., and Riahi, S., "RETRACTED: Al2O3 nanoparticles in concrete and different curing media", ***Energy and Buildings***, Vol. 43, No. 6, (2011), 1480–1488. doi:10.1016/j.enbuild.2011.02.018
22. Mosalman, S., Rashahmadi, S., and Hasanzadeh, R., "The Effect of TiO_2 Nanoparticles on Mechanical Properties of Poly Methyl Methacrylate Nanocomposites", ***International Journal of Engineering, Transactions B: Applications***, Vol. 30, No. 5, (2017), 807–813. doi:10.5829/idosi.ije.2017.30.05b.22
23. Nazari, A., Riahi, S., Riahi, S., Shamekhi, S. F., and Khademno, A., "Influence of Al_2O_3 nanoparticles on the compressive strength and workability of blended concrete Enhancing the adhesion of diamond-like carbon films to steel substrates using silicon-containing interlayers View project Influence of Al_2O_3 nanoparticles ", ***Journal of American Science***, Vol. 6, No. 5, (2010), 6–9.
24. Sobolev, K., Flores, I., Hermosillo, R., and Torres-Martínez, L. M., "Nanomaterials and Nanotechnology for High-Performance Cement Composites", Proceedings of ACI Session on Nanotechnology of Concrete: Recent Developments and Future Perspectives, (2006), 91–118.
25. Joshaghani, A., Balapour, M., Mashhadian, M., and Ozbakkaloglu, T., "Effects of nano-TiO_2, nano-Al_2O_3, and nano-Fe_2O_3 on rheology, mechanical and durability properties of self-consolidating concrete (SCC): An experimental study", ***Construction and Building Materials***, Vol. 245, (2020), 118444. doi:10.1016/j.conbuildmat.2020.118444
26. Meddah, M. S., Praveenkumar, T. R., Vijayalakshmi, M. M., Manigandan, S., and Arunachalam, R., "Mechanical and microstructural characterization of rice husk ash and Al_2O_3 nanoparticles modified cement concrete", ***Construction and Building Materials***, Vol. 255, (2020), 119358. doi:10.1016/j.conbuildmat.2020.119358
27. Li, Z., Wang, H., He, S., Lu, Y., and Wang, M., "Investigations on the preparation and mechanical properties of the nano-alumina reinforced cement composite", ***Materials Letters***, Vol. 60, No. 3, (2006), 356–359. doi:10.1016/j.matlet.2005.08.061
28. Oltulu, M., and Şahin, R., "Effect of nano-SiO_2, nano-Al_2O_3 and nano-Fe2O3 powders on compressive strengths and capillary water absorption of cement mortar containing fly ash: A comparative study", ***Energy and Buildings***, Vol. 58, (2013), 292–301. doi:10.1016/j.enbuild.2012.12.014
29. Behfarnia, K., and Salemi, N., "The effects of nano-silica and nano-alumina on frost resistance of normal concrete", ***Construction and Building Materials***, Vol. 48, (2013), 580–584. doi:10.1016/j.conbuildmat.2013.07.088
30. Ismael, R., Silva, J. V., Carmo, R. N. F., Soldado, E., Lourenço, C., Costa, H., and Júlio, E., "Influence of nano-SiO_2 and nano-Al2O3 additions on steel-to-concrete bonding", ***Construction and Building Materials***, Vol. 125, (2016), 1080–1092. doi:10.1016/j.conbuildmat.2016.08.152
31. Niewiadomski, P., Stefaniuk, D., and Hoła, J., "Microstructural Analysis of Self-compacting Concrete Modified with the Addition of Nanoparticles", ***Procedia Engineering***, Vol. 172, (2017), 776–783. doi:10.1016/j.proeng.2017.02.122
32. Ghazanlou, S. I., Jalaly, M., Sadeghzadeh, S., and Korayem, A. H., "A comparative study on the mechanical, physical and morphological properties of cement-micro/nanoFe_3O_4 composite", ***Scientific Reports***, Vol. 10, No. 1, (2020), 1–14. doi:10.1038/s41598-020-59846-y
33. Heidarzad Moghaddam, H., Maleki, A., and Lotfollahi-Yaghin, M. A., "Durability and Mechanical Properties of Self-compacting Concretes with Combined Use of Aluminium Oxide Nanoparticles and Glass Fiber", ***International Journal of Engineering, Transaction A: Basics***, Vol. 34, No. 1, (2021), 26–38. doi:10.5829/ije.2021.34.01a.04
34. Zeinolabedini, A., Tanzadeh, J., and Mamodan, M. T., "Laboratory Investigation of Ultra-High–Performance Fiber-Reinforced Concrete Modified with Nanomaterials", ***Journal of Testing and Evaluation***, Vol. 49, No. 1, (2021), 20180806. doi:10.1520/JTE20180806
35. Muzenski, S., Flores-Vivian, I., and Sobolev, K., "Hydrophobic modification of ultra-high-performance fiber-reinforced composites with matrices enhanced by aluminum oxide nano-fibers", ***Construction and Building Materials***, Vol. 244, (2020), 118354. doi:10.1016/j.conbuildmat.2020.118354
36. Faez, A., Sayari, A., and Manie, S., "Mechanical and Rheological Properties of Self-Compacting Concrete Containing Al2O3 Nanoparticles and Silica Fume", ***Iranian Journal of Science and Technology, Transactions of Civil Engineering***, Vol. 44, No. S1, (2020), 217–227. doi:10.1007/s40996-019-00339-y
37. Self-Compacting Concrete European Project Group, The European guidelines for self-compacting concrete: Specification, production and use. International Bureau for Precast Concrete (BIBM), (2005).
38. ASTM Standard C39/C39M-18, Standard test method for compressive strength of cylindrical concrete specimens, ASTM International, West Conshohocken PA, (2018).
39. ASTM Standard C496/C496M-17 Standard test method for splitting tensile strength of cylindrical concrete specimens, ASTM International, West Conshohocken PA, (2017).
40. ASTM C642-13, Standard Test Method for Density, Absorption, and Voids in Hardened Concrete, ASTM International, West Conshohocken, PA, (2013).
41. Hibbitt, H., Karlsson, B., and Sorensen, E., 'ABAQUS user's manual.' Providence, RI: Dassaulat Systems Simulia Corp, (2016).
42. ASTM Standard C33/C33M-18, Standard specification for concrete aggregates. ASTM International, West Conshohocken

PA, (2018).

43. Hosen, M. A., Jumaat, M. Z., Alengaram, U. J., and Ramli Sulong, N. H., "CFRP strips for enhancing flexural performance of RC beams by SNSM strengthening technique", ***Construction and Building Materials***, Vol. 165, (2018), 28–44. doi:10.1016/j.conbuildmat.2017.12.052

Persian Abstract

چکیده

در مطالعه حاضر به بررسی آزمایشگاهی و عددی مقاوم‌سازی تیرهای بتن مسلح، با استفاده از روکش‌های بتنی مسلح با بتن خودتراکم حاوی نانو ذرات اکسید آلومینیوم و میکروسیلیس پرداخته شد. مطالعه آزمایشگاهی در دو مرحله انجام شد. در مرحله اول، به بررسی خواص بتن تازه (جریان اسلامپ، T50، قیف V، جعبه L) و خواص بتن سخت شده (مقاومت‌های فشاری، کششی و خمشی، جذب آب) حاوی نانوذرات آلومینیوم (۰ تا ۳ درصد وزنی سیمان) و میکروسیلیس (۱۰ درصد وزنی سیمان) پرداخته شد. پس از بررسی مشخصات بتن تازه و سخت شده حاوی نانو ذرات آلومینیوم و تعیین بهینه‌ترین طرح (با توجه به آزمایش‌های انجام شده) به بررسی مقاوم‌سازی تیرهای بتن مسلح با استفاده از روکش‌های بتنی مسلح با بتن خودتراکم حاوی نانو ذرات آلومینیوم و میکروسیلیس پرداخته شد. برای این منظور پنج تیر بتن مسلح ۱/۴ متری با ابعاد و مشخصات فولادگذاری یکسان ساخته شدند و در حالت‌های با و بدون مقاوم‌سازی تحت بارگذاری چهار نقطه‌ای قرار گرفتند. در روکش بتنی یکبار از بتن معمولی و بار دیگر از بتن حاوی نانو ذرات اکسید آلومینیوم (بهینه ترین طرح) استفاده شد. روکش‌های بتنی یکبار در تمام سطوح پیرامونی و پایین تیرها و بار دیگر ۷۵ درصد سطوح پیرامونی و پایین آنها را پوشش دادند. پس از اتمام مراحل آزمایشگاهی، تیرهای بتن مسلح مطابق با شرایط آزمایشگاه با استفاده از روش اجزاء محدود و نرم افزار ABAQUS شبیه‌سازی شدند. پس از حصول اطمینان از دقت روش در شبیه‌سازی بکار برده شده، تحلیل پارامتریک انجام شد و پارامترهایی نظیر طول دهانه تیر (۱/۵، ۳، ۴/۵ متر)، ضخامت روکش بتنی (۴، ۸ و ۱۲ سانتی‌متر) و قطر میلگردهای استفاده شده در روکش (۸، ۱۰ و ۱۲ میلی‌متر) مورد بررسی قرار گرفت. نتایج حاصل از تحلیل اجزاء محدود تیرها نشان داد که استفاده از روکش‌های بتنی مسلح حاوی نانوذرات آلومینیوم بسته به ضخامت روکش، تعداد میلگردهای مورد استفاده در روکش و طول دهانه تیر، طاقت خمشی تیرها را حدوداً به مقدار ۱۵۵ تا ۴۴۷ درصد افزایش داده است. خرد شدن پوشش بتنی یکی از مسائل متداول در عناصر سازه‌ای بتنی می‌باشد. در این مطالعه مشاهده شده است که خرد شدگی بتن بدون نانوذرات در مقایسه با بتن حاوی نانوذرات شدید است، زیرا نانوذرات ماتریس بتن را تحت تاثیر قرار می‌دهد و خرد شدگی آن را کاهش می‌دهند.